EBioMedicine 37 (2018) 521–534

Contents lists available at ScienceDirect

EBioMedicine

journal homepage: www.ebiomedicine.com

EBioMedicine
Published by THE LANCET

An acellular bioresorbable ultra-purified alginate gel promotes intervertebral disc repair: A preclinical proof-of-concept study

Takeru Tsujimoto [a], Hideki Sudo [b,*], Masahiro Todoh [c], Katsuhisa Yamada [a], Koji Iwasaki [a], Takashi Ohnishi [a], Naoki Hirohama [c], Takayuki Nonoyama [d], Daisuke Ukeba [a], Katsuro Ura [a], Yoichi M. Ito [e], Norimasa Iwasaki [a]

[a] Faculty of Medicine and Graduate of Medicine, Department of Orthopedic Surgery, Hokkaido University, N15W7, Sapporo, Hokkaido 060-8638, Japan
[b] Faculty of Medicine and Graduate of Medicine, Department of Advanced Medicine for Spine and Spinal Cord Disorders, Hokkaido University, N15W7, Sapporo 060-8638, Hokkaido, Japan
[c] Faculty of Engineering, Division of Human Mechanical Systems and Design, Hokkaido University, N13W8, Sapporo, Hokkaido 060-8628, Japan
[d] Faculty of Advanced Life Science, Division of Advanced Transdisciplinary Sciences, Hokkaido University, N21W11, Sapporo, Hokkaido 001-0021, Japan
[e] Department of Biostatistics, Graduate School of Medicine, Hokkaido University, N15W7, Sapporo, Hokkaido 060-8638, Japan

ARTICLE INFO

Article history:
Received 18 September 2018
Received in revised form 14 October 2018
Accepted 23 October 2018
Available online 30 October 2018

Keywords:
Intervertebral disc
Biomaterials
Biomechanics
Tissue engineering

ABSTRACT

Background: The current surgical procedure of choice for lumbar intervertebral disc (IVD) herniation is discectomy. However, defects within IVD produced upon discectomy may impair tissue healing and predispose patients to subsequent IVD degeneration. This study aimed to investigate whether the use of an acellular bioresorbable ultra-purified alginate (UPAL) gel implantation system is safe and effective as a reparative therapeutic strategy after lumbar discectomy.
Methods: Human IVD cells were cultured in a three-dimensional system in UPAL gel. In addition, lumbar spines of sheep were used for mechanical analysis. Finally, the gel was implanted into IVD after discectomy in rabbits and sheep *in vivo*.
Findings: The UPAL gel was biocompatible with human IVD cells and promoted extracellular matrix production after discectomy, demonstrating sufficient biomechanical characteristics without material protrusion.
Interpretation: The present results indicate the safety and efficacy of UPAL gels in a large animal model and suggest that these gels represent a novel therapeutic strategy after discectomy in cases of lumbar IVD herniation.
Fund: Grant-in-Aid for the Ministry of Education, Culture, Sports, Science, and Technology of Japan, Japan Agency for Medical Research and Development, and the Mochida Pharmaceutical Co., Ltd.

1. Introduction

Lumbar intervertebral disc (IVD) herniation is a primary cause of unilateral leg pain and the most common cause of daily living limitation in individuals younger than 45 years of age [1,2]. Discectomy is performed to remove IVD material and relieve the pain inflicted by nerve root compression. However, the defect within IVD produced by discectomy may not readily heal, which may predispose patients to further IVD degeneration. As a result, there is the potential for reherniation and recrudescence of symptoms, which can necessitate additional surgery [3]. Surgeons may therefore resort to excessive IVD removal (with the aim of preventing further herniation), by extracting even intact elements within the IVD [3]. Although this strategy may lower the risk of reherniation, published data indicate that IVD degeneration subsequently intensifies, resulting in worse clinical outcomes and long-term back pain [3–5].

The IVD has two components: the nucleus pulposus (NP, the interior structure) and the annulus fibrosus (AF, the outer layer). NP is rich in glycosaminoglycans, proteoglycans, and type II collagen, and it is highly hydrated, such that physiologic osmotic pressures readily dissipate any mechanical forces transmitted through the spine [6]. Because IVD degeneration is marked by a loss of hydration in, and degradation of, the NP extracellular matrix [6], a promising strategy for restoring IVD functions in less advanced degenerative states has been NP regeneration [7–10]. However, the regeneration capacity of IVDs is limited, as viable cells capable of replicating a tissue-specific phenotype are scarce in the IVD [11]. In addition, although an IVD in a live animal experiences dynamic loading during daytime, thereby enhancing the transport of nutrients and waste products [12], poor nutritional supply to the cells of the avascular IVD is one of the inherent obstacles to IVD regeneration [9,10,13].

Biological methods of IVD repair have gained interest as alternatives to NP regeneration [14–16]. The use of injectable defect-filing hydrogels for IVD tissue implantation has been attempted in fundamental and translational research [14,17–21]. However, precursor hydrogel

* Corresponding author.
E-mail address: hidekisudo@yahoo.co.jp (H. Sudo).

https://doi.org/10.1016/j.ebiom.2018.10.055

Research in context

Evidence before this study

The use of injectable defect-filing hydrogels for osteochondral defect has been attempted in fundamental and translational research. Especially, fundamental research in this area has shown that alginate promotes osteochondral repair. However, the high concentration of endotoxins is undesirable for a medical material retained in the human body. We have developed an acellular bioresorbable ultra-purified alginate (UPAL) gel implantation system. The gel is highly purified with reduced endotoxicity (<1/10,000 compared to conventional alginate) that could be used for any biomedical or clinical applications. Our previous studies showed that UPAL gel enhanced osteochondral repair in a rabbit model.

Added value of this study

As a similar lesion of chondral defect, there is a defect within intervertebral disc (IVD) produced by discectomy for lumbar IVD herniation. Currently, there are no clinically available hydrogels for use in discectomy-associated defects, because they may be extruded due to high intradiscal pressure before the congelation. Our implantation strategy uses $CaCl_2$ surface coverage for rapid curing of the alginate gel, which then conforms to variously shaped defects without covering or suturing the surface of the IVD. In this study, the UPAL gel showed sufficient biomechanical properties without material protrusion after discectomy. In addition, we show that UPAL gel promotes IVD repair in translational models of IVD degeneration and that the UPAL-based approach is safe and does not elicit toxic effects based on International Organization for Standardization and Good Laboratory Practice standards.

Implications of all the available evidence

This preclinical proof-of-concept study shows the potential safety and efficacy of UPAL gel as an acellular endogenous reparative therapeutic strategy after discectomy that shows superiority to discectomy alone. Given that there are no current therapies for the repair of IVD defects produced by discectomy, our novel therapeutic strategy presented here has clinical potential. We are now conducting a first-in-human clinical trial in patients with lumbar IVD herniation.

injections normally congeal under body temperature, and they may be extruded due to high intradiscal pressure before the congelation [7]. There have been no exhaustive biomechanical investigations of hydrogels using clinically relevant loads, such as those assessing metallic spinal implants in the context of daily human activity, which are thought to be essential for regulatory review process.

Alginate is an anionic polysaccharide distributed in the cell walls of brown algae and is widely used as a pharmaceutical additive. Sodium alginate is the sodium salt of alginate; it remains in the sol condition in aqueous solution and can be gelated by the addition of $CaCl_2$. This character has been applied for human mesenchymal stem cell proliferation and chondrogenic differentiation in a three-dimensional (3D) alginate scaffold [22,23]. In addition, fundamental research in this area has shown that alginate promotes IVD repair [16,17,24]. However, the high concentration of endotoxins found in this naturally occurring gel is undesirable for a medical material retained in the human body. Commercial-grade alginates have been shown to contain 10–20 mitogenic impurities, which include natural substances and bacterial contaminants that incite immunogenic reactions [25]. In addition, the non-thermoresponsive nature of alginate hydrogel, which is normally polymerized *in vitro* before *in vivo* implantation, is an issue for clinical application. An efficient mechanism for the *in vivo* delivery of alginate hydrogel remains an unmet need in this setting [7].

There are no clinically available hydrogels for use in discectomy-associated defects, and there is still a need for innovation in terms of clinical safety and efficacy. Here, we report the use of an acellular bioresorbable ultra-purified alginate (UPAL) gel implantation system to prevent post-discectomy IVD degeneration. The UPAL gel is highly purified with reduced endotoxicity (<1/10,000 compared to conventional alginate) that could be used for any biomedical or clinical applications [26–28]. In addition, our implantation strategy uses $CaCl_2$ surface coverage for rapid curing (~5 min) of the alginate gel, which then conforms to variously shaped defects without covering or suturing the AF. The *in situ* forming gel has potential effects regarding *in vivo* delivery of the alginate, thereby potentially reducing the risk of extrusion of the material. Although a high concentration of calcium ions is known to strengthen the alginate gel, exposed cells are then at risk of apoptosis [29]. Reducing the cytotoxicity of $CaCl_2$ would be ideal in this circumstance. In addition, $CaCl_2$ can be easily washed away after gelation. We show that this novel treatment led to reparative tissue proliferation and improved IVD water content in a rabbit and sheep model of discectomy. Sheep are widely used in both biomechanical and material implantation preclinical models because of their bioanatomic similarities to humans [19,30,31]. We have developed a good manufacturing practice (GMP) formulation that is now positioned for first-in-human clinical trials.

2. Materials and methods

2.1. Study design

Animal models were designed to assess whether acellular UPAL gel provides a biomatrix scaffolding suitable for IVD repair after discectomy and to investigate the potential reparative mechanisms entailed in UPAL gel implantation. The primarily explored parameters were: (i) potential IVD cell viability, apoptosis, and proliferation in 3D alginate composites; (ii) biomechanical properties of functional spinal units (FSUs; vertebra-IVD-vertebra) after UPAL gel implantation; (iii) reparative capacity of degenerative IVDs *in vivo*; (iv) biologic safety testing after UPAL gel implantation, examining systemic and local toxicities; and (v) potential mechanisms of IVD repair *via* UPAL gel implantation.

The ethics committee of the Hokkaido University Graduate School of Medicine (Hokkaido, Japan) approved the use of human IVDs. Animal procedures incorporated were approved by the Institutional Animal Care and Use Committee at Hokkaido University, Hamri Co., Ltd., and Hatano Research Institute.

Rabbit (male Japanese white rabbit; age, 20 weeks; weight, 2.8–3.5 kg) and sheep (male Suffolk sheep; age, 2 years; weight, 40–60 kg) models were used. The sample size for the rabbit model was determined for each of the three time points used here through previous studies [8,9]. For the sheep model, we performed a power analysis on the basis of our preliminary study (unpublished data). The treatments were randomized across scientific team members who performed the surgical procedures and postsurgical care. The surgical procedures were performed by one surgeon. Three IVDs (two in rabbits and one in sheep) were excluded owing to surgical complications. The treatments were randomized and blinded from team members who performed the surgical procedures and postsurgical care.

2.2. Preparation of human NP cells

Human NP samples were obtained from T12-L1, L1-L2, and L2-L3 levels (total 27 IVDs) from nine patients (mean age ± standard deviation, 15.3 ± 3.3 years) who underwent anterior spinal fusion for adolescent idiopathic scoliosis in Hokkaido University Hospital. The samples were taken during the surgical procedure. Before surgery, all IVDs were analysed by MRI and graded for degenerative changes using the

Pfirrmann classification system [32]. All IVDs were grade 1, suggesting that all the samples were non-degenerated IVDs.

The cells were isolated from the human NP samples and cultured as previously described [8,9,33]. Briefly, each gel-like NP was separated from AF under a dissecting microscope. The tissue specimens were placed in a complete culture medium containing Dulbecco's modified Eagle's medium (DMEM; Sigma-Aldrich, St. Louis, MO, USA, glucose concentration; 4.5 mg/ml) supplemented with 10% foetal bovine serum (FBS; Nichirei Bioscience, Tokyo, Japan), 1% penicillin/streptomycin, and 1.25 mg/ml fungizone (Life Technologies, Thermo Fisher Scientific, Waltham, MA, USA). The preparations were washed twice by centrifugation (1000 rpm, 3 min) and resuspended in DMEM supplemented with 0.25% collagenase (no.032–22,364, Wako Pure Chemical Industries). For cell isolation, the preparations were incubated in a shaking incubator (2%O_2, 5% CO_2, 37 °C, 4 h) and then centrifuged twice (1000 rpm, 3 min). Cells that were separated from the matrix were placed in 10-cm tissue culture dishes and incubated in a humidified atmosphere (2%O_2, 5% CO_2, 37 °C, 4–6 weeks).

2.3. Preparation of alginate gel and 3D NP cell-alginate composites

UPAL gel (Mochida Pharma Co. Ltd., Tokyo, Japan) at two viscosities was prepared (LV-UPAL, 100–200 mPa/s; and NV-UPAL, 400–600 mPa/s) in addition to CAL (sodium alginate, #199–09961, 400–600 mPa/s, Wako Pure Chemical Industries, Osaka, Japan). Alginate in seaweed was extracted *via* conversion to water-soluble sodium alginate. Caustic soda was added to extract sodium alginate from swollen seaweed. The aqueous alginate solution was then isolated *via* a clarification procedure. As this aqueous alginate solution was highly viscous, this solution was diluted with large quantities of water prior to clarification. This processing stage utilizes proprietary unpublished know-how technology. Seaweed extract was then filtered to separate sodium alginate solution from fibrous seaweed residue.

To isolate alginic acid from diluted sodium alginate solution, an acid was added. In an acidic system, insoluble alginic acid was precipitated and isolated. The acid precipitation method is also based on know-how technology and is particularly suitable to produce high-quality alginic acid. The viscosity values were established by the manufacturer. The mannuronic acid/guluronic acid (M/G) ratio of the alginates was 1.0:1.4. For the *in vitro* and *in vivo* studies, we used sodium alginate solution (2% *w/v*) [16,17] dissolved in phosphate-buffered saline (PBS; Wako Pure Chemical Industries) and 102 mM $CaCl_2$ for all three groups. The endotoxin level of UPAL was 5.76 EU/g and that of CAL was 75,950 EU/g [26]. After two passages, the NP cells were dissociated from monolayers and encapsulated in 3D alginate beads [34] for *in vitro* experiments.

2.4. Cell viability and apoptosis analysis

At 2, 7, 14, and 28 days after encapsulation, live and dead cells were detected using calcein-AM cell-permeant dye and propidium iodide (PI) (Dojindo, Kumamoto, Japan) and confocal laser-scanning microscopy (Fluoview FV300; Olympus, Tokyo, Japan). Counts of live and dead cells in the beads were obtained manually. Four fields, each containing at least 15 cells, were counted in each area [33,35]. Additionally, 3D NP cell–alginate composites were dissolved in 55 mM sodium citrate (4 °C) until the beads and cells were separated for subsequent labelling (using an Annexin–Fluorescein Isothiocyanate (FITC) Apoptosis Detection Kit II; BD Biosciences, Franklin Lakes, NJ, USA). Both early apoptotic cells ($FITC^+PI^-$) and late apoptotic cells ($FITC^+PI^+$) were monitored *via* flow cytometry (BD Biosciences), and the results were combined during analysis [9].

2.5. Cell proliferation assay

At 3 h and at 3 or 7 days after encapsulation, alginate beads were dissolved in 50 mM ethylenediaminetetraacetic acid (EDTA). Viable cells were counted at each time point (Cell Counting Kit-8 [CCK-8]; Dojindo) as per the manufacturer's protocol. Cell viability was measured by using a microplate reader (Bio-Rad, Life Sciences Research, Hercules, CA, USA) at 450-nm wavelength [26].

2.6. Serum starvation

At 7 days after encapsulation, human NP cells were washed with PBS, followed by two washes in DMEM to remove any remaining culture medium, and the cells were then incubated at 37 °C, 5% CO_2, and 20% O_2 in serum-deprived medium, which consisted of DMEM supplemented with 1% penicillin/streptomycin and 1.25 mg/mL fungizone. Because our prior work showed that significant NP cell apoptosis occurs 48 h after serum starvation [10], the cells were harvested and analysed at 48 h after serum withdrawal. NP cells that were not subjected to serum starvation served as untreated controls. Serum starvation leads to *in vitro* IVD degeneration [9,10,33]. At two time points (6 h and 48 h) after serum starvation, cell viability and apoptosis analyses were performed using confocal laser-scanning microscopy and flow cytometry, respectively.

2.7. Unconfined compression tests

UPAL and CAL gel (diameter, 4.5 mm; thickness, 2 mm) were subjected to unconfined compression testing [7,36], which was performed using a tensile-compressive mechanical tester (AutographAG-X; Shimadzu, Kyoto, Japan). The gels were compressed at a constant speed of 0.5 mm/min, and Young's moduli were derived from linear regions between 10% and 20% compression strain of stress/strain curves (4 gels per group). These unconfined tests did not mimic the IVD; however, they were used to assess the mechanical properties of UPAL gels compared to those of CAL gels.

2.8. Biomechanical testing

Lumbar (L) spines of 15 sheep were used for biomechanical testing; 8 sheep were randomly selected for static loading experiments, and 7 were randomly selected for dynamic loading experiments. L1-L2, L3-L4, and L5-L6 FSUs were cut out from each spine and cast in polyester resin moulds (Ostron II; GC Corp, Tokyo, Japan), with reinforcement by 3-mm diameter screws [37]. Supraspinous and interspinous ligaments were transected, whereas intertransverse ligaments and transverse processes were preserved.

For the static loading test, left-sided unilateral facetectomy and partial discectomy were performed. Partial discectomy represented transection of the posterior longitudinal ligament and posterior aspect of AF combined with removal of the NP [38]. This procedure is based on standard clinical surgical technique for lumbar IVD herniation, therefore, the model is suitable to evaluate whether the UPAL gel herniates from the IVD and to evaluate biomechanical behavior of the gel in the clinical setting.

An AF incision (5 mm width × 3 mm height) was made [39], and 0.20 g of NP was removed from each disc. The AF incision is equivalent to 8 mm width × 8.5 mm height in adult human IVDs [40]. To confirm that UPAL gel does not herniate under more severe IVD defects, double the amount of NP was removed relative to that in the previous *in vivo* sheep model [39,41,42]. The vertebrae were not decompressed to facilitate injection of the gel. The UPAL solution (150–250 μl) was injected into FSUs in the UPAL gel group after discectomy without pressurization; 102 mM $CaCl_2$ solution was then injected on top of the UPAL solution for gelation, and biomechanical testing was performed 1 h later. The specimens were placed onto a dual column table top model testing system (Model 5943; Instron Corp, Norwood, MA, USA), and a preconditioning load was applied for compression loading. Preconditioning lasted several minutes up to −300 N (minus indicates compression loading) at a constant speed (1 mm/min). Thereafter, the specimens

were released from the preload before applying the other load, followed by assessment of bilateral axial rotation (±6 Nm), in turn followed by bilateral axial rotation, flexion, extension, and bilateral bending tests (±6 Nm) in sequence [37,38]. The levels of the moments were selected on the basis of previous nondestructive biomechanical tests using cadaveric lumbar spine segments to assess physiologic movements in the specimen [37,38,43,44]. Finally, compression loading (up to −1000 N) was assessed at a constant speed (1 mm/min) [45,46]. The compression loading of 1000 N in sheep IVD is equivalent to the pressure on human lumbar IVDs when lifting a weight of 20 kg with a rounded back posture [45,46]. Compression stiffness was calculated on the basis of the linear regression of the load-displacement curve between 60% and 100% of the maximal load [21] or between −400 N and −600 N [47]. Because the present biomechanical characteristics were assessed under a physiological range of load in the context of daily human activity, analysis of breaking strength, such as load under which the FSU or IVD collapses, was not performed to measure the strength of the IVD. The range of motion measurements under flexion–extension and bilateral bending was recorded as the angle change in a testing jig that was previously reported [37].

For the dynamic axial loading test, a sinusoidal load between −300 N and 300 N was applied for 1000 cycles at 1 Hz after −300 N preloading, using the Instron Model 5943 instrument, as described previously [19]. Specimens were released from the preload before application of the dynamic load. A tensile force on FSUs is not applied *in vivo*; however, only two previous studies have performed a dynamic axial loading test, using a hydrogel [19,20] and we reviewed previous studies [19,20] to evaluate stiffness during the dynamic loading test. Although the previous studies limited the cycle range to 20 cycles (±300 N at 1 Hz) [19,20], we selected a larger number of cycles considering clinically relevant cycles in the context of daily human activity, wherein an individual stoops down 10 times per day to the day of approximate disappearance period of the gel (100 days). Compression stiffness was calculated from linear regression of the load displacement between −200 N and− 300 N at 1000 cycles (6 or 7 FSUs per group) [19].

2.9. In vivo validation in rabbit and sheep IVD degeneration model

Currently, there are no clinically available alginates comparable with the UPAL gel. In addition, we previously reported that implantation of the UPAL gel significantly improved the reparative tissue of osteochondral defects compared to the CAL gel in a rabbit model [26]. Hence, we did not include the CAL gel arm in our *in vivo* trials from the standpoint of animal protection.

Forty rabbits were used for *in vivo* UPAL gel implantation. Of these rabbits, 24 were randomly selected for qualitative analysis of IVD degeneration (MRI, histology, and IHC), and a total of 70 IVDs were randomly allocated for IVD degeneration analysis of the intact control, aspirated alone, and UPAL gel groups (7 or 8 discs per group). The remaining 16 rabbits were used for qualitative analysis of $GD2^{+}Tie2^{+}$ cells, which are NP progenitor cells [48] using frozen sections of rabbit NPs; a total of 48 IVDs were randomly allocated to the three groups described above.

Under general anaesthesia (pentobarbital sodium, 30 mg/kg) and local anaesthesia (1% lidocaine), the spine was located *via* a retroperitoneal approach. AF punctures were performed using 18-gauge needles, aspirating the NPs using 10-ml syringes at the L2/3 and L4/5 IVDs. L3/4 IVDs were left intact as controls. In the UPAL gel group, IVD defects were filled with UPAL solution (20 μl) using a microsyringe (Hamilton Medical, Switzerland) and a 25-gauge needle. Then, 102 mM $CaCl_2$ (1 ml) was injected on top of the UPAL solution for gelation. Five minutes later, the operative wound was irrigated with normal saline and closed. Rabbits were sacrificed by intravenous injection of overdosed pentobarbital at 4, 12, and 24 weeks after surgery for analysis of IVD degeneration or at 2 and 4 weeks after surgery for qualitative analysis of $GD2^{+}Tie2^{+}$ cells.

For the sheep model, the *in vivo* study was not performed under GLP regulation; however, all procedures were performed in a medical product GLP-adapted laboratory (Hamri Co., Ltd., Ibaraki, Japan). Twenty-one sheep were used for qualitative analysis of IVD degeneration. A total of 83 IVDs were randomly allocated to the intact control (7 discs), discectomy alone (10 discs), and UPAL gel (10 or 11 discs) groups. After preliminary intramuscular medication (xylazine, 0.2 mg/kg; ketamine, 20 mg/kg), maintenance narcosis was achieved by inhalation anaesthesia (isoflurane). All of the sheep were operated on *via* a right lateral retroperitoneal approach, and each disc was subjected to standard microdiscectomy. An AF incision (5 × 3 mm) was made [39], and 0.10 g of NP was removed from each IVD [39,41,42]. In the UPAL gel group, disc defects were filled with UPAL solution (100–200 μl) and injected with 102 mM $CaCl_2$ solution (3 ml) on top of the UPAL solution, as for the rabbit model. The volume of UPAL solution depends on disc preparation. The sheep were sacrificed by intravenous injection of overdosed pentobarbital at 4, 12, and 24 weeks after surgery.

2.10. MRI analysis

T2-weighted midsagittal images of the IVDs were obtained using a 7.0-T MR scanner (Varian Unity Inova; Varian Medical Systems, Palo Alto, CA, USA) for the rabbit model [8,9] and a 3.0-T MR scanner (MAGNETOM Prisma; Siemens, Munich, Germany) for the sheep model. The Pfirrmann classification scheme was applied to grade IVD degeneration [32]. Quantitative analysis was also performed to determine the MRI index using Analyze software v10.0 (AnalyzeDirect, Overland Park, KS, USA) [8,9]. All image assessments were performed by three independent observers who were blinded to the samples, and the mean of the three evaluations was recorded.

2.11. Histological analysis

After MRI analysis, each IVD was processed for IHC staining. Midsagittal sections (5-μm thick) were stained routinely (using haematoxylin and eosin; H&E) or using safranin O-fast green for evaluation of proteoglycan expression. The discs were evaluated semi-quantitatively and graded from 0 (normal) to 5 (highly degenerative) [49,50] in the rabbit model and from 0 (normal) to 36 (highly degenerative) [51] in the sheep model. For appropriate evaluation for each rabbit and sheep IVD, different grading systems were used in each animal model. All image assessments were performed by three independent blinded observers, and the mean of the three evaluations was recorded.

2.12. IHC analysis

IHC staining was performed to detect collagen type I and II (not procollagen type I and II forms) (rabbit, sheep), alginate (rabbit, sheep), GD2 (rabbit), and Tie2 (rabbit). For GD2 and Tie2 staining, NP tissues were embedded in optimum cutting temperature (OCT) compound (Sakura Finetek, Tokyo, Japan) and snap-frozen in liquid nitrogen before fixing them in 4.0% paraformaldehyde (4 °C, 5 min) for sectioning. To prevent NP tissues from spreading into the fixing solution, before sectioning, paraformaldehyde was applied on the whole-frozen (in OCT) samples.

For the rabbit model, mouse monoclonal antibodies to type I collagen (1:100; Sigma-Aldrich, C2456), type II collagen (1:50; Daiichi Fine Chemical, F-57, Tokyo, Japan), or GD2 (1:100; Abcam, ab68456, Cambridge, UK), a goat monoclonal antibody to alginate (1:40 Mochida, CPK-K TB1364), and a goat polyclonal antibody to human Tie2 (1:20; R&D systems, AF313, Minneapolis, MN, USA) were applied. Sections intended for collagen type I and II staining and for alginate staining were deparaffinized in xylene and rehydrated. For IHC of collagen type I and type II, sections were pretreated (15 min) with proteinase K (Dako, Agilent Technologies, Santa Clara, CA, USA), which was not

required for IHC to detect alginate. After washing with PBS, sections were treated for 30 min with 1% H_2O_2 in methanol and then incubated with primary antibody for 60 min at room temperature (for type II collagen) or overnight at 4 °C (for type I collagen, alginate, GD2, and Tie2). Sections were then incubated for 30 min in peroxidase (EnVision+ System Kit; Dako) (for type I collagen, type II collagen, alginate, and GD2) or in biotinylated anti-goat IgG + Vectastain ABC kit (Vector USA, Torrance, CA, USA) (for Tie2). Staining was developed using 3,3′-diaminobenzidine hydrochloride (Dako) and Mayer's haematoxylin (Merck, Darmstadt, Germany) as a counterstain. For alginate staining, rabbit NP tissue at 7 days after *in vivo* UPAL gel implantation was used as a positive control, and NP tissue lacking the primary antibody was used as a negative control. Intact rabbit NP tissue (GD2) and a blood vessel in a rabbit muscle (Tie2) were used as positive controls, and the specimens that were not treated with a primary antibody were used as negative controls (Supplementary Fig. 1).

For fluorescence staining, both anti-GD2 and anti-Tie2 were applied immediately after paraformaldehyde fixation. Then, Alexa-Fluor-568-conjugated donkey anti-mouse-IgG (Invitrogen, Thermo Fisher Scientific, A10037) and FITC-conjugated AffinoPure F-Fragment donkey anti-goat-IgG (Jackson ImmunoResearch, 705–096-147, West Grove, PA, USA) were used as secondary antibodies. Cells positive for type I or type II collagen were separately counted in five independent, randomly selected fields [9]; $GD2^+Tie2^+$ cells were counted in all fields of glass slides. Values are expressed as percentages of positive cells relative to total cell counts. All experiments were performed on eight IVDs from each treatment group and at each time point.

For the sheep model, goat antibody to type I collagen (1:40; Southern Biotech, Birmingham, 1310–01, AL, USA), a mouse monoclonal antibody to type II collagen (1:100; Daiichi Fine Chemical, F-57), and a goat monoclonal antibody to alginate (1:40; Mochida, CPK-K TB136) were used. The sections were deparaffinized in xylene and rehydrated. After washing with PBS, they were treated for 10 min with 3% H_2O_2 in methanol, after which protein blocking was undertaken (Protein Block Serum-Free; Dako). Blocking was not needed for alginate staining. The sections were incubated for 60 min at room temperature with primary antibody and for 30 min with peroxidase (EnVision+ System kit; Dako) (for type I collagen and alginate) or Histofine Simple StainMax-PO (Nichirei Biosciences, Burlingame, CA, USA) (for type II collagen). Staining was developed using 3,3′-diaminobenzidine hydrochloride (Dako) and Mayer's haematoxylin as a counterstain. Cells positive for type I or type II collagen were separately counted, as described above.

2.13. Biological safety testing

The safety testing was performed at Hatano Research Institute, Food and Drug Safety Center (Kanagawa, Japan), in accordance with "Basic Principles of Biological Safety Evaluation Required for Application for Approval to Market Medical Devices" (Pharmaceutical and Food Safety Bureau, Japanese Ministry of Health, Labour and Welfare, Notification Yakushokuki-hatsu 0301 No. 20, March 1, 2012), "Biological Evaluation of Medical Devices - Part 1: Evaluation and Testing within a Risk Management Process" (ISO 10993-1, October 15, 2009), "Biological Evaluation of Medical Devices - Part 6: Tests for Local Effects after Implantation" (ISO 10993-6, April 15, 2007), and "Biological Evaluation of Medical Devices - Part 11: Tests for Systemic Toxicity" (ISO 10993-11, August 15, 2006) and in compliance with the Japanese Ministry of Health, Labour and Welfare Ordinance No. 37 "Good Laboratory Practice Standard Ordinance for Nonclinical Laboratory Studies on Safety of Medical Devices" (March 23, 2005; partially revised by Japanese Ministry of Health, Labour and Welfare Ordinance No. 115, June 13, 2008, and Ordinance No. 87, July 30, 2014).

Briefly, the L2/3 and L4/5 IVDs of 36 rabbits were aspirated, and UPAL gel implantation was performed (UPAL gel group) as described above. To evaluate systemic toxicity, we measured body weight changes once every week, food consumption once every week, and haematological and blood biochemical profiles at 26 weeks after surgery and performed urinalysis at 26 weeks after surgery. Weights of principal organs such as heart, lung, and so forth were obtained, along with pathologic examinations and histological assessments (H&E) at 26 weeks after surgery (12 rabbits per group). Histologic assessments (H&E and safranin O staining) of the IVDs were also performed at 4 and 26 weeks after surgery (6 rabbits per group). Tissues were examined for the following: (i) inflammatory response (types of inflammatory cells and degree of infiltration); (ii) presence or absence of fibrous capsule and capsular components; (iii) degeneration or necrosis and proliferation of adipose tissue; (iv) haemorrhage and neovascularization; and (v) test sample residues [52].

2.14. Statistical analysis

Sample sizes for the quantitative data in preclinical studies were determined by power analysis using one-way ANOVA, an α level of 0.05, power of 0.8, and effect size of 1.60. All data are expressed as the means ± standard error (SEM). One-way ANOVA, two-way ANOVA, and Tukey-Kramer tests were applied for multigroup comparisons. Unpaired Student's *t*-test or Pearson's chi-squared test were invoked for two-group comparisons. We carried out randomization of samples and were blinded to the samples being tested. All statistical computations were performed in JMP Pro v13.0 statistical software (SAS Institute, Cary, NC, USA) with a significance threshold of $p < .05$.

3. Results

3.1. Effects of UPAL gel on human NP cell viability

Although UPAL gel is intended as an acellular vehicle, it is important to understand its biocompatibility with human NP cells for its potential clinical use, compared to the traditional commercial-grade alginate that was used in the experimental *in vitro* study. We therefore first investigated the impact of UPAL gel (Supplementary Fig. 2) on human NP cells. Non-degenerate human NP cells obtained from human donors were suspended in UPAL gel or commercial-grade alginate gel (CAL) solution (2% *w*/*v*), and gels were then formed by $CaCl_2$. Because the viscosity of CAL gel was 400–600 mPa/s, we prepared same viscosity for the UPAL gel as a normal viscosity UPAL gel (NV-UPAL gel). In addition, low viscosity (LV-) UPAL gel (viscosity:100–200 mPa/s) was used to investigate the effects of viscosity on NP cell viability. The resultant 3D NP cell–alginate gel beads were then cultured for 28 days before assessing NP cell viability, apoptosis, and proliferation using confocal laser-scanning micrographs (CLSM) or flow cytometry (FCM). Whereas CLSM measured the percentage of viable cells, FCM could distinguish viable cells from dead or apoptotic cells. Therefore, early phenotypic changes in NP cells could be assessed *via* FCM [10]. We did not observe any significant differences in cell viability or apoptosis at various time points between the CAL gel, LV-UPAL gel, and NV-UPAL gel groups (Fig. 1a–e, Supplementary Fig. 3). Similarly, the degrees of cell proliferation in the CAL gel, LV-UPAL gel, and NV-UPAL gel groups at 3 h, 2 days, and 7 days after encapsulation did not differ significantly (Supplementary Fig. 3f).

We then tested UPAL gel in an established *in vitro* model of degenerated IVD [9,10,33]. To simulate nutrient deprivation of NP cells, which leads to IVD degeneration, human NP cells in 3D alginate composites were cultured for 7 days and then serum-starved for 48 h [9,10,33]. Previous reports have demonstrated that serum starvation of NP cells for 48 h is likely to have a sufficient effect for degeneration after 7 days of exposure to 10% serum [9,10,33]. The LV-UPAL gel and NV-UPAL gel groups showed no significant differences in NP cell viability or apoptosis in subsequent CLSM (Supplementary Fig. 4a and b) or FCM (Supplementary Fig. 4c–e). Based on these results, and our expectation that the more viscous NV-UPAL gel would be easier for surgeons

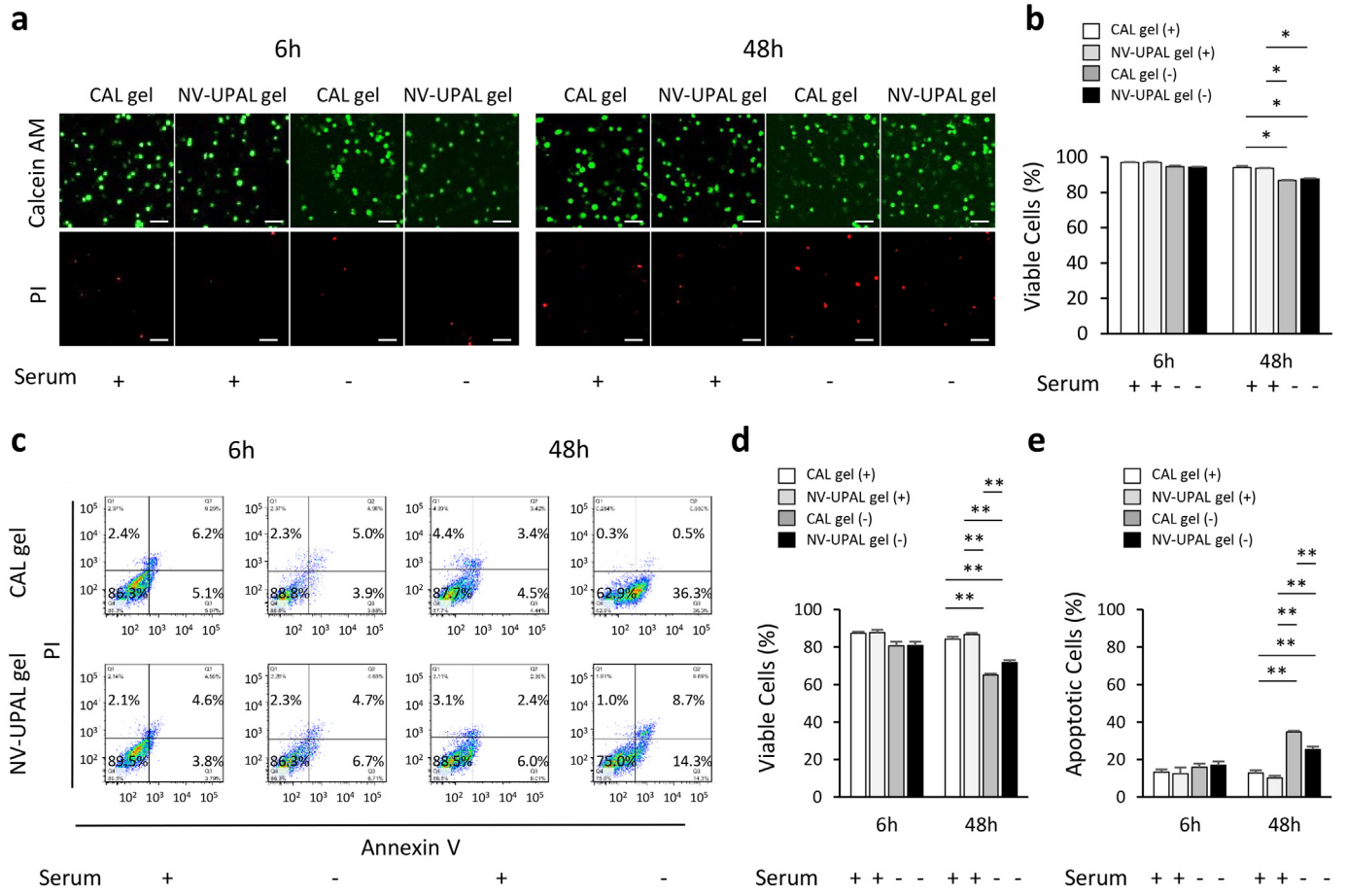

Fig. 1. Human NP cells in 3D UPAL gel composites were viable in serum-starved conditions. (a) Confocal laser-scanning micrographs of three-dimensional (3D) nucleus pulposus (NP) cell–alginate gel composites (commercial-grade alginate; CAL, normal viscosity ultra-purified alginate; NV-UPAL) at 6 and 48 h after serum starvation and staining with calcein AM (green) and propidium iodide (PI) (red). Five replicates were tested, and representative images are shown. Scale bar, 100 μm. (b) Cell viability determined by counts of live and dead cells in confocal laser-scanning micrographs. (*$p < 0.05$, Tukey-Kramer test). (c) Flow cytometry scatter plots. Five replicates were tested, and representative images are shown. Both early apoptotic cells ($FITC^+$ PI^-) and late apoptotic cells ($FITC^+$ PI^+) were monitored *via* flow cytometry. FITC, fluorescein isothiocyanate. (d and e) Longitudinal evaluation of cell viability (d) and apoptosis (e). Data are from five independent experiments (means ± SEM). *p < 0.05, **$p < 0.01$ between indicated groups; p values were determined by one-way ANOVA with *post hoc* Tukey-Kramer test. The plus signs indicate groups incubated in a complete culture medium, and the minus signs indicate groups incubated in serum-starved conditions. h, hours.

to handle in the operating room, NV-UPAL gel was utilized in the ensuing experiments.

Comparisons of the NV-UPAL gel and CAL gel groups using CLSM showed no significant differences in viability (Fig. 1a and b, Supplementary Table 1). However, a significantly higher percentage of viable cells ($p = .0019$, Tukey-Kramer test) and a lower percentage of apoptotic cells ($p = .0007$, Tukey-Kramer test) were evident in the NV-UPAL gel group relative to the CAL gel group using FCM at 48 h after onset of serum starvation (Fig. 1c–e, Supplementary Table 1). The overall results of these *in vitro* experiments suggest that the UPAL gel has higher biocompatibility with human NP cells compared to the commercial-grade alginate gel.

3.2. UPAL gel showed sufficient biomechanical characteristics without material protrusion after discectomy

We next investigated the mechanical properties of UPAL gel using unconfined compression tests which is the most popular mechanical testing configuration to measure the mechanical properties of cylindrical hydrogel samples. In UPAL gel and CAL gel disc-shaped fabrications (diameter, 4.5 mm; thickness, 2 mm) for unconfined compression detection [7,36], the ratio of longitudinal stress to strain for UPAL gel (18.5 ± 4.6 kPa) and CAL gel (18.8 ± 4.2 kPa), representing Young's moduli, were similar to one another and to the ratios of normal human NP tissue [36] (Supplementary Fig. 5a and b).

Next, we conducted *in vitro* non-destructive biomechanical testing using cadaveric sheep FSUs. Each FSU was randomly allocated for intact control, discectomy alone, and UPAL gel groups. After standard partial discectomy was performed (see methods section), the UPAL solution was injected into a single FSU in the (NV-) UPAL gel group after discectomy; 102 mM $CaCl_2$ solution was then injected on top of the UPAL solution for gelation, and biomechanical testing was performed 1 h later. Static testing was performed by applying compressive loads or enacting movements in six directions, using load/movement ranges tested in previous biomechanical models of lumbar reconstruction that reflect daily human activity [38,47,53]. For the dynamic axial loading test, a sinusoidal load between −300 N and 300 N at 1 Hz [19] was applied for 1000 cycles.

No herniation of UPAL gel was macroscopically observed throughout static loading tests involving all FSUs (Fig. 2a). There was no significant difference in the compression stiffness or exerted movements in six directions among the intact control, discectomy alone, and UPAL gel groups (Fig. 2b–f, Supplementary Table 2). No herniation of UPAL gel was observed throughout the dynamic loading tests in any of the FSUs (Fig. 2g). The compression stiffness in the discectomy group was significantly lower than that in the intact control group, whereas the UPAL gel partially restored the stiffness relative to the intact control group

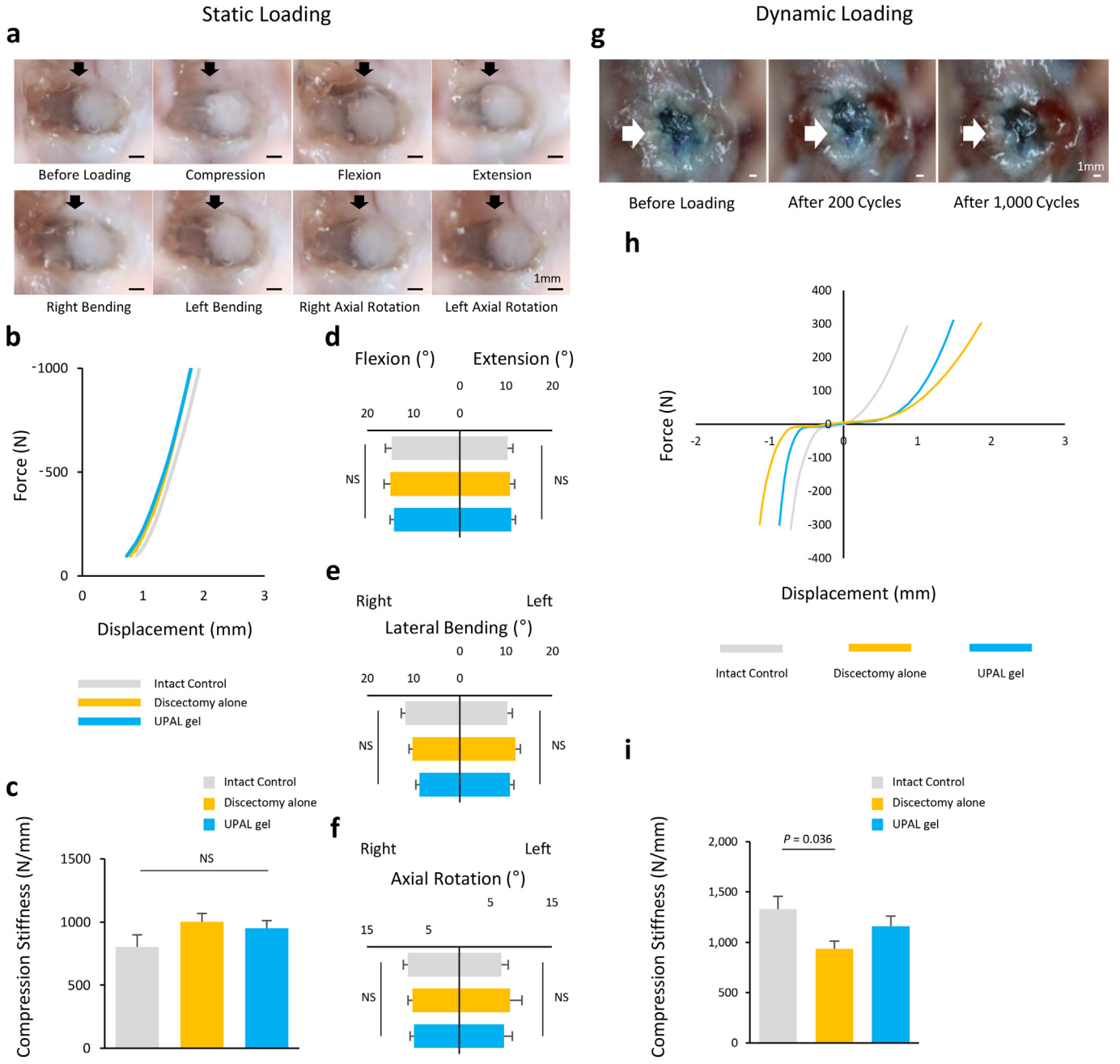

Fig. 2. UPAL gel showed sufficient biomechanical properties without material protrusion after discectomy. We conducted *in vitro* non-destructive biomechanical testing using cadaveric sheep functional spinal units (FSUs; vertebra-IVD-vertebra). (a) Photographs of implanted ultra-purified alginate (UPAL) gel before loading and after static loading testing. Images are representative of 8 replicates. Scale bar, 1 mm. (b) Load-displacement curve under axial compression. (c) Compression stiffness between −400 N and −600 N. Data are means ± SEM. (d) Range of motion (ROM) in flexion and extension tests. (e) Bilateral bending test. (f) Bilateral axial rotation test. (g) Photographs of a representative implanted gel before loading after the 200th and 1000th load cycle. Six or seven replicates were tested, and representative images are shown. UPAL gel was stained with toluidine blue for visibility. Scale bar, 1 mm. (h) Load-displacement curve at the 1000th cycle under axial loading. (i) Compression stiffness between −200 N and −300 N. Throughout, data are represented as mean ± SEM. P was determined by one-way ANOVA with *post hoc* Tukey-Kramer test. NS, not significant.

(Fig. 2h and i). These results indicate that UPAL gel implantation had sufficient biomechanical effects without material protrusion after discectomy under clinically relevant loads in the context of daily human activity.

3.3. UPAL gel preserves the water content of IVDs compared to discectomy alone in rabbits and sheep

We next attempted to regenerate IVD using UPAL gel *in vivo* in rabbit and sheep models. We chose these models to assess the efficacy of UPAL gel, overcoming the differences in animal species. In the rabbit model, a total of 70 IVDs from 24 adult rabbits were randomly allocated to the intact control (7 or 8 discs), aspirated alone (8 discs), and UPAL gel (8 discs) groups. In the sheep model, 83 discs from 21 skeletally mature sheep were randomly allocated to the intact control (7 discs), discectomy alone (10 discs), and UPAL gel (10 or 11 discs) groups. Briefly, rabbit or sheep discs were surgically exposed by a lateral retroperitoneal approach (see method section). After NP aspiration (rabbit) or discectomy (sheep), the disc cavities were filled with UPAL solution; $CaCl_2$ was subsequently injected on top of the UPAL fill solution for

gelation (Supplementary Fig. 6, Supplementary Movie 1). Five minutes later, the operative wound was irrigated with normal saline and closed.

Degenerative changes in rabbit lumbar IVDs were analysed qualitatively by magnetic resonance imaging (MRI), capturing T2-weighted, midsagittal images (Fig. 3a). IVD degeneration was scored according to the Pfirrmann classification [32] on a 5-point scale, combining signal loss and loss of height of the IVDs (grade 5 was categorized as severely degenerated). The MRI index (the product of the NP area and the average signal intensity) [8,9] was used to calculate degenerative change of the NP. Signal intensities diminished over time in the surgically removed IVDs and were higher in the UPAL gel group than in the aspirated alone group. The Pfirrmann grades in the UPAL gel group were significantly lower ($p < .0001$, Tukey-Kramer test) than those in the aspirated alone group (Fig. 3b). In addition, the MRI index in the UPAL gel group was significantly higher ($p < .0001$, Student's *t*-test) than that in the aspirated alone group (Fig. 3c). Sheep lumbar IVDs were also analysed to qualitatively assess degenerative changes (Fig. 3d). The Pfirrmann grades in the UPAL gel group were significantly lower ($p = .0377$, Tukey-Kramer test) than those in the discectomy alone group (Fig. 3e). Furthermore, the MRI index in the UPAL gel group was significantly higher ($p = .0310$, Student's t-test) than that in the discectomy alone group (Fig. 3f). These MRI assessments suggest that UPAL gel preserved the water content of IVDs compared to discectomy alone.

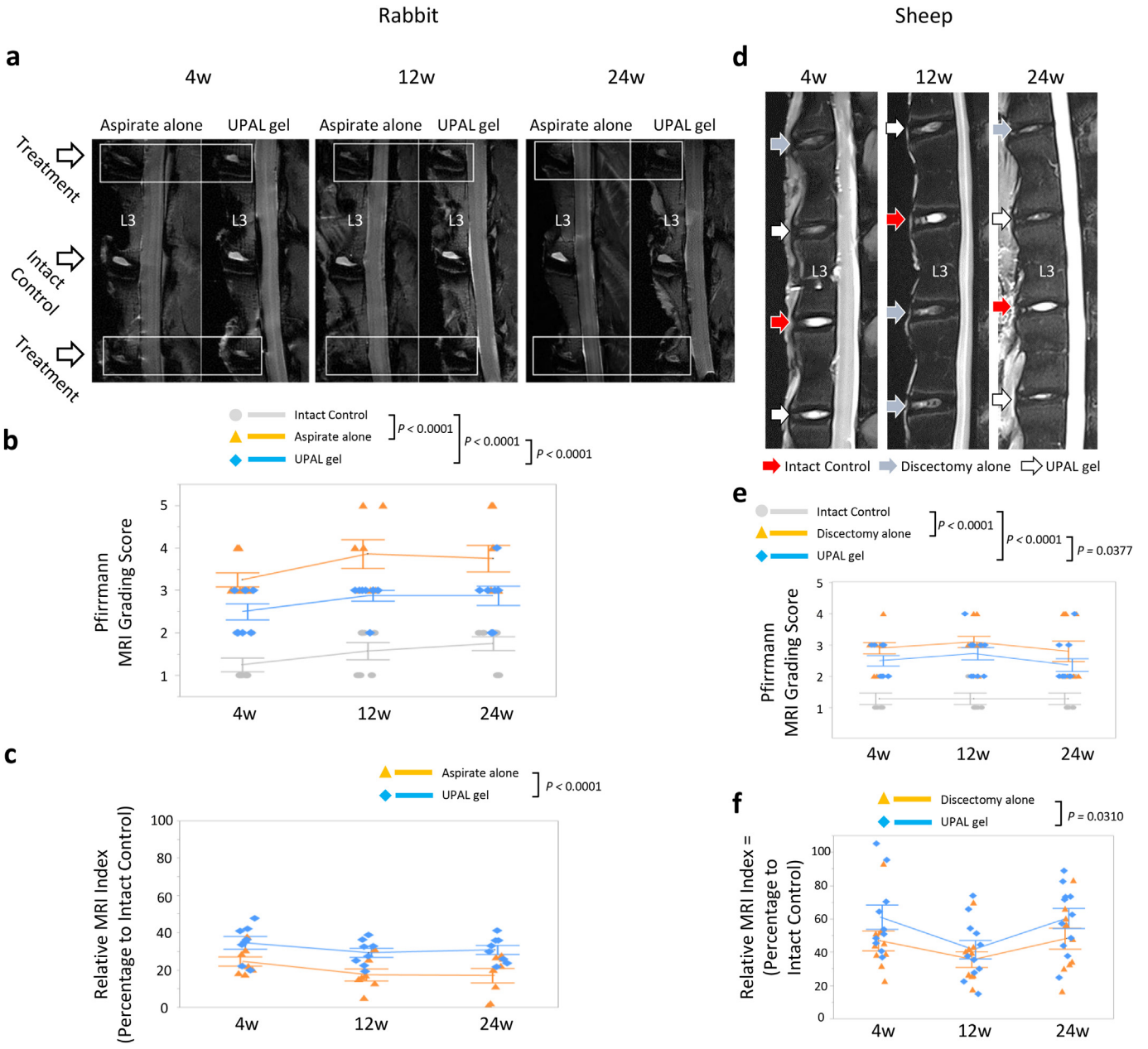

Fig. 3. UPAL gel preserved water content of IVDs after discectomy. (a) T2-weighted, midsagittal images of intervertebral discs (IVDs) at 4, 12, and 24 weeks after surgery in rabbits. Images are representative of 7 or 8 replicates. (b) Pfirrmann grading of IVD degeneration. Data are means ± SEM (intact control, $n = 7$; 12 weeks or 8; 4 and 24 weeks; aspirate alone, n = 7; 12 weeks or 8; 4 and 24 weeks; UPAL gel, $n = 8$). UPAL, ultra-purified alginate. (c) Magnetic resonance imagining (MRI) index (nucleus pulposus (NP) area × average signal intensity) for degenerative alterations of the NP. Numerical values expressed as percentages, compared with intact control IVDs. Data are means ± SEM. (d) Representative T2-weighted, midsagittal images of IVDs at 4, 12, and 24 weeks after surgery in sheep. (e and f) Pfirrmann grading (e) and MRI index (f) are shown. Data are means ± SEM (intact control, n = 7; discectomy alone, $n = 10$; UPAL gel, n = 10; 4 weeks or $n = 11$; 12, 24 weeks). P was determined by two-way ANOVA with *post hoc* analysis using the Student's *t*-test (c, f) or the Tukey-Kramer test (b, e). w, weeks.

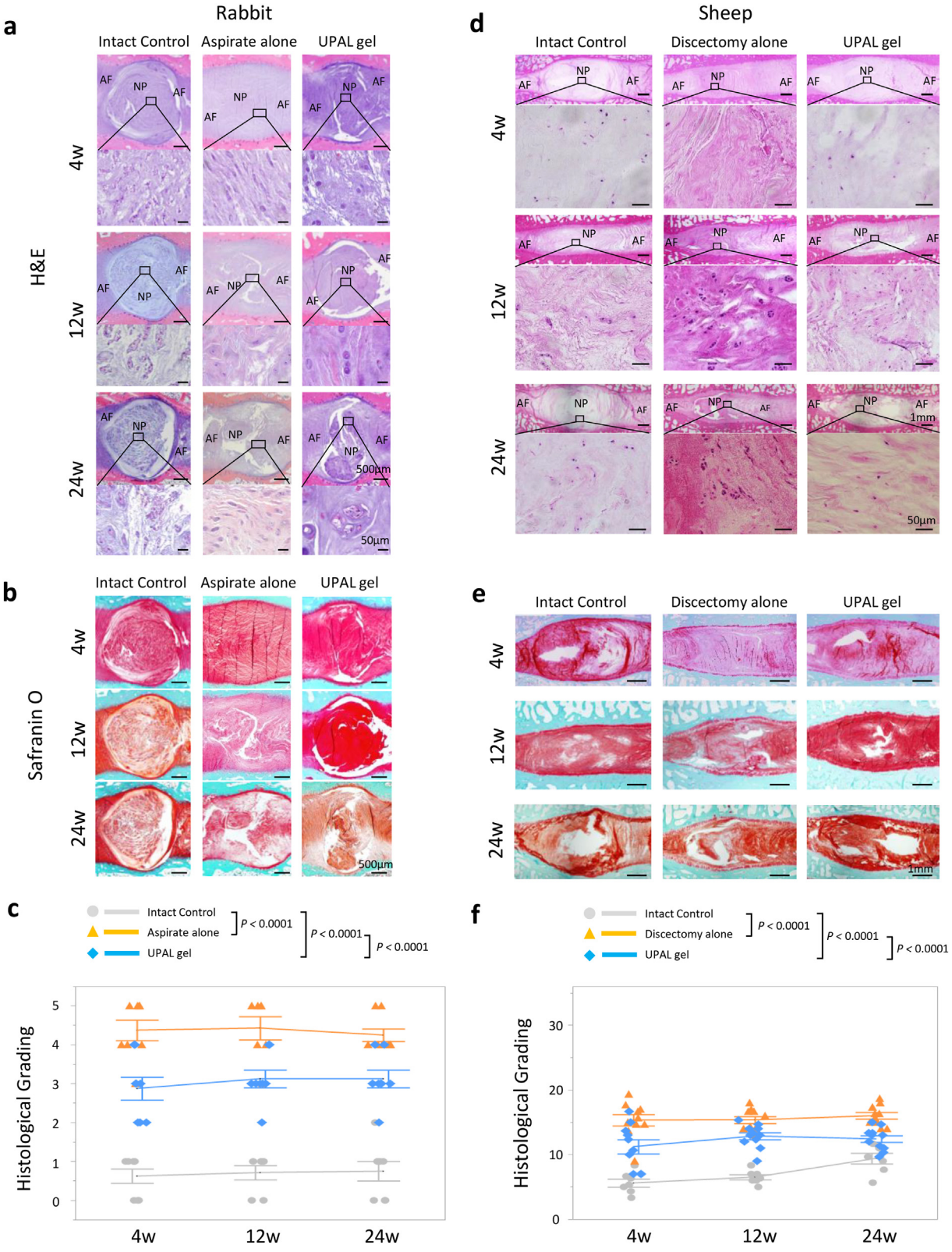

Fig. 4. UPAL gel prevented IVD degeneration after discectomy. (a and b) Midsagittal sections of rabbit intervertebral discs (IVDs) stained by Haematoxylin and Eosin (H&E) (a) or safranin O (b). Images are representative of 7 or 8 replicates (intact control, n = 7; 12 weeks or 8; 4 and 24 weeks; aspirate alone, n = 7; 12 weeks or 8; 4 and 24 weeks; UPAL gel, n = 8). UPAL, ultra-purified alginate. AF; annulus fibrosus, NP; nucleus pulposus. Scale bar, (a); 50 μm (second, fourth, and sixth sections from the top) or 500 μm (first, third and fifth sections from the top) (b); 500 μm. (c) Histological grading is shown. Data are means ± SEM. (d and e) Midsagittal sections of sheep IVDs stained by H&E (d) or safranin O (e). Representative images are shown (intact control, n = 7; discectomy alone, n = 10; UPAL gel, n = 10; 4 weeks or n = 11; 12 and 24 weeks). Scale bar, (d); 50 μm (second, fourth, and sixth sections from the top) or 1 mm (first, third, and fifth sections from the top) (e); 1 mm. (f) Histological grading is shown. Data are means ± SEM. *P* values in (c) and (f) were determined by two-way ANOVA with *post hoc* Tukey-Kramer test. w, weeks.

3.4. UPAL gel prevents IVD degeneration after discectomy in rabbits and sheep

The UPAL gel was not visible in MR images (data not shown). However, because the injected UPAL gel is highly hydrophilic, it would presumably result in greater hyperintense regions upon T2-weighted imaging than in the surrounding tissue; hence, we also performed histological evaluation of the IVDs. In rabbits, intact control specimens had typical, oval-shaped NPs, with no structural collapse of the inner AF (Fig. 4a and b). In aspirated alone specimens, the inner AF was collapsed, and fibrotic changes of NPs were observed at all of the time points examined. However, the inner AFs of UPAL gel-treated specimens appeared relatively well preserved, with minimal fibrosis of NPs (Fig. 4a and b). Accordingly, the scoring of degeneration in the UPAL gel group, as assessed by histology, was significantly lower ($p < .0001$, Tukey-Kramer test) than that in the aspirated alone group (Fig. 4c). As in the sheep model, scar formation or granulation tissue increased over time in the IVDs of the discectomy alone group (Fig. 4d and e), whereas the IVDs of the UPAL gel group showed less degeneration (Fig. 4d). Histologic degeneration scores in the UPAL gel group were significantly lower ($p < .0001$, Tukey-Kramer test) than those in the discectomy alone group (Fig. 4f). These results suggest that UPAL gel prevented IVD degeneration compared to discectomy alone.

3.5. UPAL gel promotes extracellular matrix production in NP in rabbits and sheep

In both the rabbit and sheep models, the percentage of type I collagen-positive NP cells was significantly lower in the UPAL gel group than in the aspirated alone ($p = .0436$, Tukey-Kramer test) or discectomy alone ($p < .0001$, Tukey-Kramer test) group (Supplementary Fig. 7a–d). In addition, the group with UPAL gel-treated IVDs harboured a significantly greater percentage ($p < .0001$, Tukey-Kramer test) of type II collagen-positive cells within NPs than the aspirated or discectomy groups (Fig. 5a–d), suggesting that UPAL gel promoted extracellular matrix production in NP that is an essential aspect of NP cell function.

3.6. UPAL gel is bioresorbable in rabbits and sheep

Immunohistochemical (IHC) staining using an anti-alginate antibody showed that alginate was present in the IVDs at 4 weeks after surgery, but that it had disappeared by 12 weeks after implantation in the rabbit model (Supplementary Fig. 8a) and by 24 weeks after implantation in the sheep model (Supplementary Fig. 8b). These results suggest that UPAL gel is a bioresorbable biomaterial.

3.7. UPAL gel is not toxic in rabbits

To evaluate the toxicity of UPAL gel not only in the implanted IVDs, but also in principal organs such as the heart, lung, *etc.*, we used a rabbit model to perform biological safety testing based on International Organization for Standardization (ISO) and Good Laboratory Practice (GLP) standards. These local and systemic evaluations are thought to be fundamental for the preclinical proof of concept (POC) test. Body weight change, food consumption, haematologic and blood biochemical profiles, and urinalysis were examined. There were no changes related to UPAL gel using this battery of tests (Supplementary Tables 3–5). Histologic examination, including inflammatory response of principal organs and IVDs, revealed no significant differences between the aspirated alone and UPAL gel groups (Supplementary Tables 6 and 7). We thus conclude that UPAL gel did not cause any systemic toxicity or injuries to tissues at implantation sites under the experimental conditions of this study.

3.8. Endogenous NP progenitor cells propagated after UPAL gel implantation

Finally, to elucidate the possible mechanism of endogenous IVD repair by UPAL gel implantation, we investigated the percentages of $GD2^{+}Tie2^{+}$ cells, which are NP progenitor cells [48]. Because antibodies specific for GD2 and Tie2 in sheep IVDs are not available, we used only rabbits. The $GD2^{+}Tie2^{+}$cells were significantly ($p < .0001$, Tukey-Kramer test) more abundant in the UPAL gel group compared to in the aspirated alone group (Fig. 6a–c). Because there were no endothelial cells in NP tissues [8–10], the observed $Tie2^{+}$ cells were not of an endothelial lineage. These results suggest that persisting NP progenitor cells were recruited and enriched by the UPAL gel, resulting in endogenous IVD repair.

4. Discussion

Because the regenerative capacity of IVDs is limited, defects created by discectomy may cause inadequate tissue healing and reherniation or may predispose patients to later IVD degeneration. In the present study, the UPAL gel shows higher biocompatibility with human NP cells than that showed by commercial-grade alginate gel and promotes extracellular matrix production, showing sufficient biomechanical characteristics without material protrusion. In addition, the UPAL gel demonstrates the lack of immunogenicity in the *in vivo* biological safety testing based on ISO and GLP standards which is an important issue, especially for translation of UPAL gel to human trials. The findings of this study underscore the potential safety and efficacy of UPAL gel as an acellular endogenous reparative therapeutic strategy after lumbar discectomy that shows superiority to discectomy alone.

We intended to confirm that the gel was not herniated under several loading conditions. In particular, the AF plays a major role under bending and torsion loading because the distance from the center of rotation is longer in AF than in NP. The present surgical procedure is based on the standard clinical surgical technique for lumbar IVD herniation; therefore partial discectomy does not result in significant loss of mechanical instability of the IVD, except for the AF defect. However, no gel herniation was observed. Subsequently, to evaluate the mechanical properties of the FSU, stiffness of the FSU was evaluated as a whole spinal unit, not as a local IVD, revealing no significant difference between discectomy alone and UPAL gel implantation.

Increasingly, researchers are pursuing stem-cell-based therapies as a means of regenerating musculoskeletal tissue, with an emphasis on the expansion and transplantation of progenitor cells [54–56]. There are many challenges in this regard, including immune rejection, pathogen transmission, potential tumourigenesis, and host tissue engraftment [54,57–59]. Matrix-based medicine offers an alternative, single-step process involving biomaterials that are cell-free and that can be stored for long periods of time, allowing on-demand treatment of IVDs after lumbar discectomy [60]. Our investigation has produced histologic evidence that the intradiscal injection of UPAL gel could suppress IVD degeneration after discectomy and significantly boost the percentage of type II collagen–positive cells, thereby promoting extracellular matrix production, which is an essential aspect of NP cell function.

In this study, the percentage of $GD2^{+}Tie2^{+}$ progenitor cells increased significantly at 2 and 4 weeks after UPAL gel implantation, although long-term assessments are lacking due to the limited availability of test rabbits. It has been speculated that vertebral bone marrow may be a source of migratory cells for degenerative IVDs [13]. However, this concept does not seem tenable, given the avascular nature of IVDs [13]. Typically, NP progenitor cells form aggregates that express type II collagen and aggrecan, and their clonal multipotency allows mesenchymal lineages to emerge for tissue reconstruction [48]. Although it is inherently nondegradable [7,61], which is presumably an asset for our purposes, the UPAL gel was not visible at week 12 in rabbits and week 24 in sheep after implantation, suggesting that it

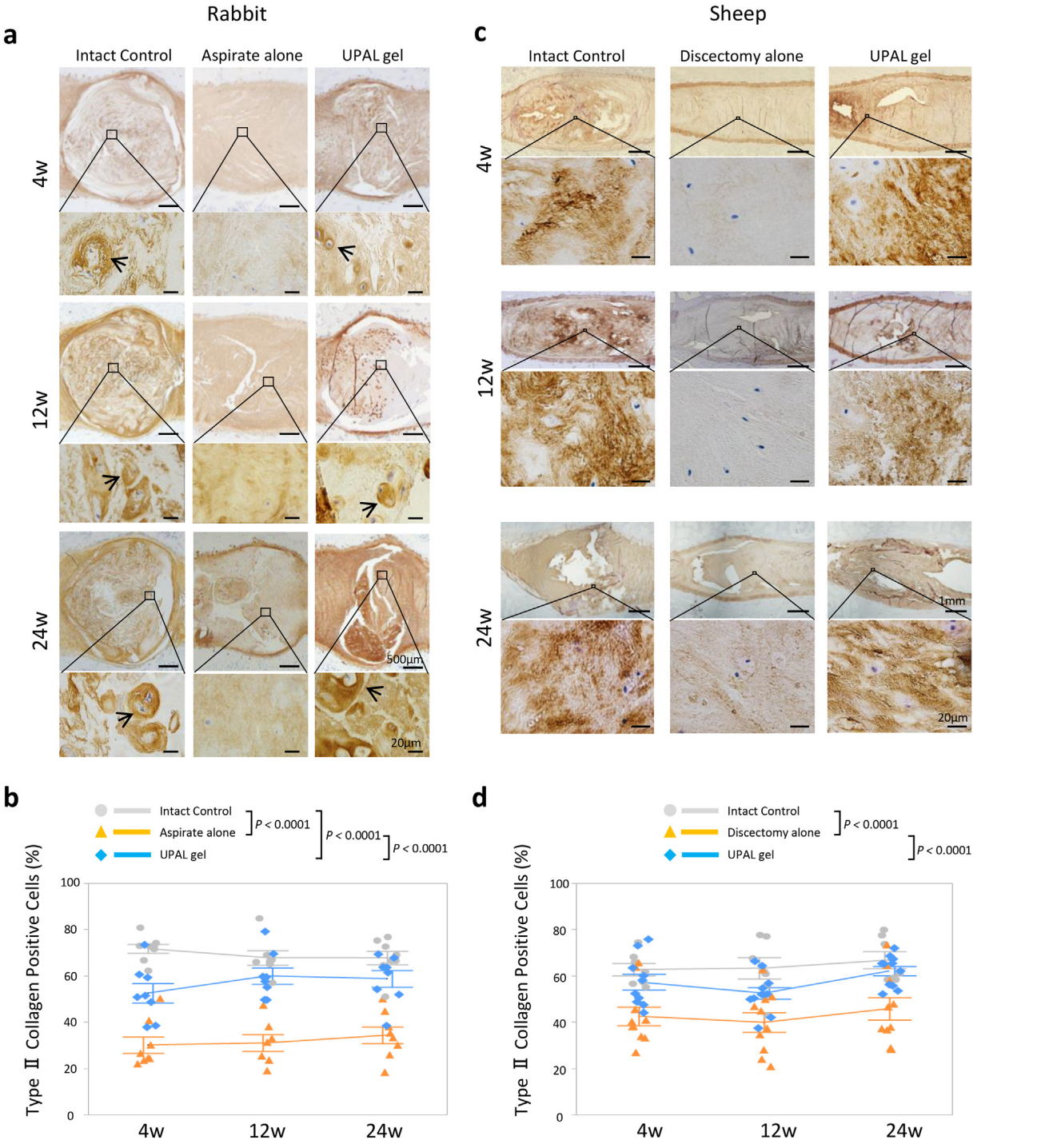

Fig. 5. Type II collagen-positive cells in rabbit and sheep NPs. (a) Midsagittal sections of rabbit intervertebral discs (IVDs) stained for type II collagen. Images are representative of 7or 8 replicates (intact control, n = 7; 12 weeks or 8; 4 and 24 weeks; aspirate alone, n = 7; 12 weeks or 8; 4 and 24 weeks; UPAL gel, n = 8). UPAL, ultra-purified alginate. Arrows indicate cells positive for type II collagen. Scale bar, 20 μm (second, fourth, and sixth sections from the top) or 500 μm (first, third, and fifth sections from the top). (b) Percentages of type II collagen-positive cells in rabbits. Data are means ± SEM. (c) Midsagittal sections of sheep IVDs stained for type II collagen. Representative images are shown (intact control, n = 7; discectomy alone, n = 10; UPAL gel, n = 10; 4 weeks or n = 11; 12 and 24 weeks). Scale bar, 20 μm (second, fourth, and sixth sections from the top) or 1 mm (first, third, and fifth sections from the top). (d) Percentages of type II collagen-positive cells in sheep. Data are means ± SEM. P values in (b) and (d) were determined by two-way ANOVA with *post hoc* Tukey-Kramer test. w, weeks.

progressively declined through physiological ion replacement (divalent to monovalent), hydrolysis, or was perhaps depleted *via* cellular encapsulation [7]. It therefore seems likely that viable endogenous NP cells migrated to post-discectomy wounds filled with UPAL; persisting NP progenitor cells were also most likely recruited and enriched in the early post-discectomy phase by the implanted biomaterial, resulting in endogenous IVD repair (Fig. 7).

Our acellular UPAL gel product can be packaged at a GMP/GLP facility and shipped to medical institutions that perform open or endoscopic discectomies. The surgeons can simply inject the biomaterial into cavitary discectomy defects. Because residual NP tissue represents a potential source of reparative cells, the quantity of NP tissue in IVDs and the magnitude of degenerative changes may impact the ability of these cells to migrate, differentiate, and aid in IVD repair [14]. We are now

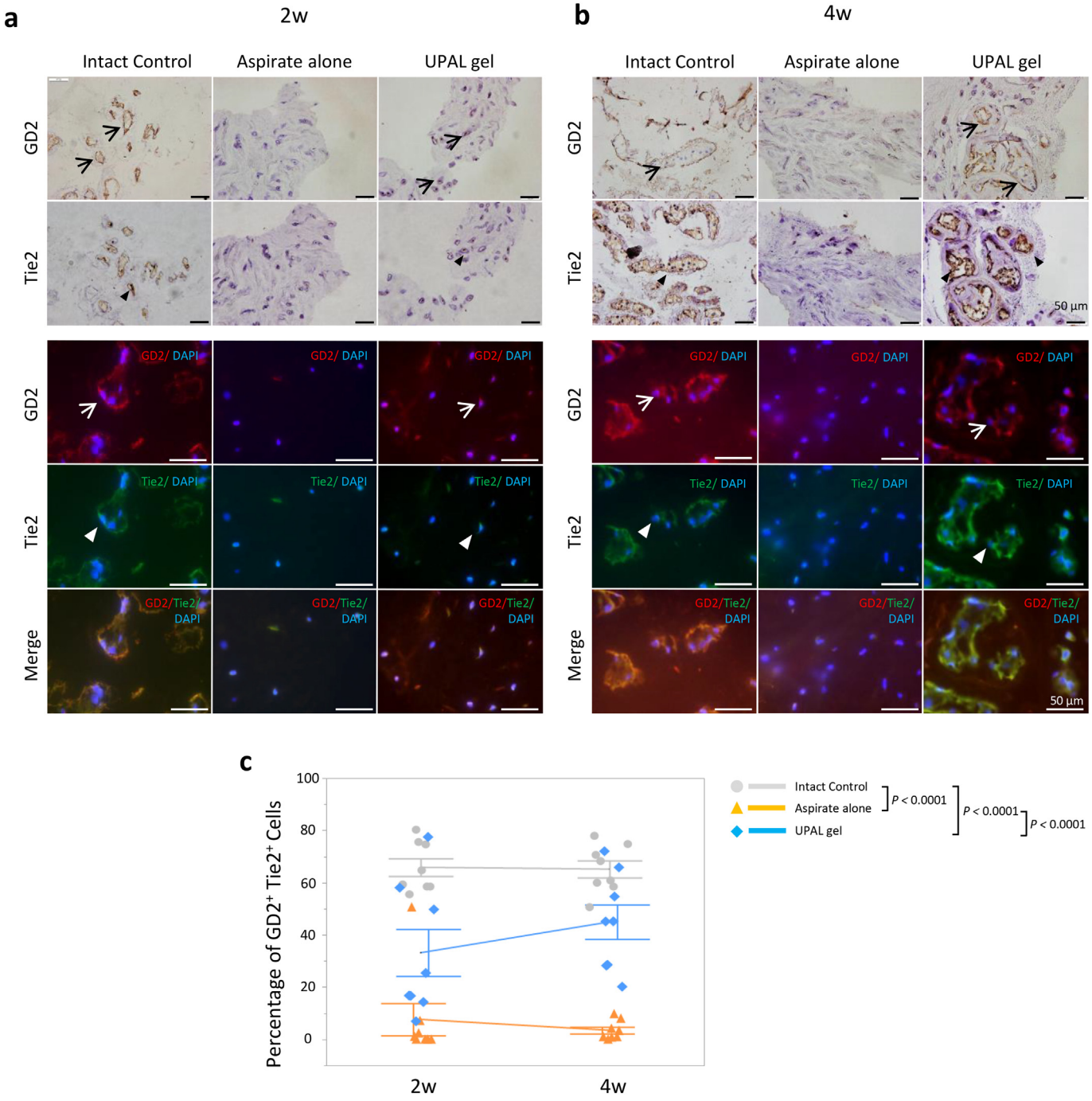

Fig. 6. Endogenous NP progenitor cells propagated after UPAL gel implantation. (a and b) Midsagittal frozen sections of rabbit intervertebral discs (IVDs) stained for GD2 and Tie2 after ultra-purified alginate (UPAL) gel implantation. GD2 and Tie2 are markers of nucleus pulposus (NP) progenitor cells. Images are representative of 8 replicates. Arrows indicate $GD2^+$ cells; arrowheads indicate $Tie2^+$ cells. Scale bars: 50 μm. GD2; red, Tie2; green, DAPI; blue. (c) Percentages of $GD2^+$ $Tie2^+$ cells. Data are means ± SEM. p was determined by two-way ANOVA with *post hoc* Tukey-Kramer test. w, weeks.

conducting a first-in-human clinical trial in which the UPAL gel will be applied for lumbar IVD herniation in young patients in their 20s–40s.

The *in vivo* models of IVD degeneration implemented in our study were generated from healthy IVDs, which might display natural healing tendencies. Healing conditions in the animal models were perfect: fresh wound, one sharp defect, no inflammation. In reality, most of the surgery are performed days or weeks after herniation (most of the times a conservative treatment is used first), thereby eliciting a strong inflammatory response and inducing degeneration (fibrosis) of NP and AF. Furthermore, the AF probably has more weak spots, similar to the contra-posterolateral area of the AF: if the gel is injected, there is a risk of reherniation on the other side of the disc. An acellular matrix-based medicine may be inappropriate in elderly population. Further *in vivo* animal investigations of product combinations, such as UPAL gel plus stem cells (*i.e.*, bone marrow mesenchymal stem cells), are needed to chronicle the course of degenerative IVDs from their onset. These further researches might address whether the UPAL gel is widely applicable even for elderly population or whether the gel is useful as a carrier for the cell therapy.

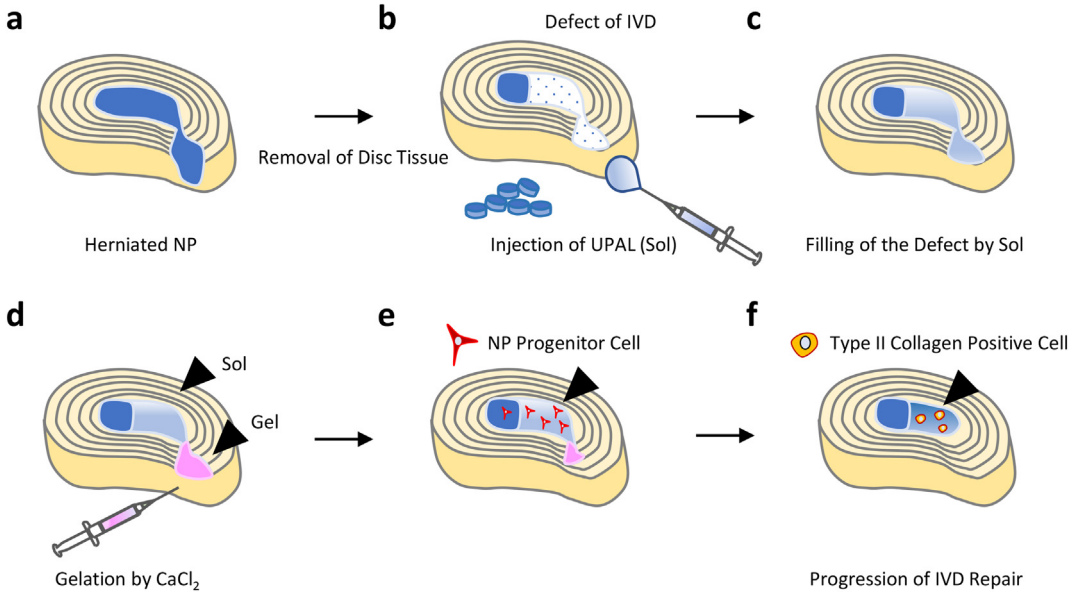

Fig. 7. Potential mechanism of IVD repair by UPAL gel implantation. (a), Schematic of herniated nucleus pulposus (NP). (b), Intradiscal ultra-purified alginate (UPAL) injection to fill post-discectomy intervertebral disc (IVD) defect. Sol; solution. (c), IVD defect filled by UPAL solution. (d), Superficial layer of UPAL solution is gelated after applying $CaCl_2$ solution. (e), Persisting NP progenitor cells are increased in UPAL composites at an early point after surgery. (f), Progressive IVD repair with differentiation of NP progenitor cells to type II collagen-positive cells.

Supplementary data to this article can be found online at https://doi.org/10.1016/j.ebiom.2018.10.055.

Acknowledgements

We would like to thank M. Isaji and S. Shimizu for material preparations and K. Maeda and F. Inage for helpful discussions. This work was supported by Grant-in-Aid for the Ministry of Education, Culture, Sports, Science, and Technology of Japan (16H03176), Japan, "Project of Translational and Clinical Research Core Centers" from Japan Agency for Medical Research and Development, AMED (16lm0103004j0005 and 18lm0203045h0001), Japan, and the Mochida Pharmaceutical Co., Ltd.

Funding sources

The sponsors of the study had no roles in study design, data collection, data analysis, data interpretation, or writing of the report. All authors had full access to all data of this study and had final responsibility for the decision to submit for publication.

Conflict of interest

Patents pertaining to this work have been filed and are pending (inventors H. S., T. T., and N. I.). The other authors declare that they have no competing interests.

Author contributions

H.S. conceived and designed the study. T.T., H.S., M.T., K.Y., K.I., T.O., N.H., T.N., D.U. and K.U. performed the experiment. T.T., H.S., N.H., T.N. and Y.M.I. analysed the results. T.T., H.S. and N.I. contributed to discussions throughout the study. T.T. and H.S. wrote and edited the manuscript.

References

[1] Andersson GB. Epidemiological features of chronic low-back pain. Lancet 1999;354(9178):581–5. https://doi.org/10.1016/S0140-6736(99)01312-4.

[2] Seki S, Kawaguchi Y, Chiba K, et al. A functional SNP in CILP, encoding cartilage intermediate layer protein, is associated with susceptibility to lumbar disc disease. Nat Genet 2005;37(6):607–12.

[3] Bailey A, Araghi A, Blumenthal S, Huffmon GV. Prospective, multicenter, randomized, controlled study of anular repair in lumbar discectomy: two-year follow-up. Spine (Phila Pa 1976) 2013;38(14):1161–9.

[4] McGirt MJ, Eustacchio S, Varga P, et al. A prospective cohort study of close interval computed tomography and magnetic resonance imaging after primary lumbar discectomy: factors associated with recurrent disc herniation and disc height loss. Spine (Phila Pa 1976) 2009;34(19):2044–51.

[5] Barth M, Diepers M, Weiss C, Thome C. Two-year outcome after lumbar microdiscectomy versus microscopic sequestrectomy: part 2: radiographic evaluation and correlation with clinical outcome. Spine (Phila Pa 1976) 2008;33(3):273–9.

[6] Frith JE, Cameron AR, Menzies DJ, et al. An injectable hydrogel incorporating mesenchymal precursor cells and pentosan polysulphate for intervertebral disc regeneration. Biomaterials 2013;34(37):9430–40.

[7] Zeng Y, Chen C, Liu W, et al. Injectable microcryogels reinforced alginate encapsulation of mesenchymal stromal cells for leak-proof delivery and alleviation of canine disc degeneration. Biomaterials 2015;59:53–65.

[8] Yamada K, Sudo H, Iwasaki K, et al. Caspase 3 silencing inhibits biomechanical overload-induced intervertebral disk degeneration. Am J Pathol 2014;184(3):753–64.

[9] Sudo H, Minami A. Caspase 3 as a therapeutic target for regulation of intervertebral disc degeneration in rabbits. Arthritis Rheum 2011;63(6):1648–57.

[10] Sudo H, Minami A. Regulation of apoptosis in nucleus pulposus cells by optimized exogenous Bcl-2 overexpression. J Orthop Res 2010;28(12):1608–13.

[11] Lee CH, Rodeo SA, Fortier LA, Lu C, Erisken C, Mao JJ. Protein-releasing polymeric scaffolds induce fibrochondrocytic differentiation of endogenous cells for knee meniscus regeneration in sheep. Sci Transl Med 2014;6(266):266ra171.

[12] Paul CP, Zuiderbaan HA, Zandieh Doulabi B, et al. Simulated-physiological loading conditions preserve biological and mechanical properties of caprine lumbar intervertebral discs in ex vivo culture. PLoS One 2012;7(3):e33147.

[13] Sakai D, Nishimura K, Tanaka M, et al. Migration of bone marrow-derived cells for endogenous repair in a new tail-looping disc degeneration model in the mouse: a pilot study. Spine J 2015;15(6):1356–65.

[14] Woiciechowsky C, Abbushi A, Zenclussen ML, et al. Regeneration of nucleus pulposus tissue in an ovine intervertebral disc degeneration model by cell-free resorbable polymer scaffolds. J Tissue Eng Regen Med 2014;8(10):811–20.

[15] Bowles RD, Williams RM, Zipfel WR, Bonassar LJ. Self-assembly of aligned tissue-engineered annulus fibrosus and intervertebral disc composite via collagen gel contraction. Tissue Eng Part A 2010;16(4):1339–48.

[16] Mizuno H, Roy AK, Vacanti CA, Kojima K, Ueda M, Bonassar LJ. Tissue-engineered composites of anulus fibrosus and nucleus pulposus for intervertebral disc replacement. Spine (Phila Pa 1976) 2004;29(12):1290–7 [discussion 7-8].

[17] Bidarra SJ, Barrias CC, Granja PL. Injectable alginate hydrogels for cell delivery in tissue engineering. Acta Biomater 2014;10(4):1646–62.

[18] Endres M, Abbushi A, Thomale UW, et al. Intervertebral disc regeneration after implantation of a cell-free bioresorbable implant in a rabbit disc degeneration model. Biomaterials 2010;31(22):5836–41.

[19] Malhotra NR, Han WM, Beckstein J, Cloyd J, Chen W, Elliott DM. An injectable nucleus pulposus implant restores compressive range of motion in the ovine disc. Spine (Phila Pa 1976) 2012;37(18):E1099–105.

[20] Gullbrand SE, Schaer TP, Agarwal P, et al. Translation of an injectable triple-interpenetrating-network hydrogel for intervertebral disc regeneration in a goat model. Acta Biomater 2017;60:201–9.

[21] Likhitpanichkul M, Dreischarf M, Illien-Junger S, et al. Fibrin-genipin adhesive hydrogel for annulus fibrosus repair: performance evaluation with large animal organ culture, in situ biomechanics, and in vivo degradation tests. Eur Cell Mater 2014;28:25–37 [discussion -8].
[22] Guo P, Yuan Y, Chi F. Biomimetic alginate/polyacrylamide porous scaffold supports human mesenchymal stem cell proliferation and chondrogenesis. Korean J Couns Psychother 2014;42:622–8.
[23] Christiansen-Weber T, Noskov A, Cardiff D, et al. Supplementation of specific carbohydrates results in enhanced deposition of chondrogenic-specific matrix during mesenchymal stem cell differentiation. J Tissue Eng Regen Med 2018;12(5):1261–71.
[24] Risbud MV, Albert TJ, Guttapalli A, et al. Differentiation of mesenchymal stem cells towards a nucleus pulposus-like phenotype in vitro: implications for cell-based transplantation therapy. Spine (Phila Pa 1976) 2004;29(23):2627–32.
[25] Zimmermann H, Zimmermann D, Reuss R, et al. Towards a medically approved technology for alginate-based microcapsules allowing long-term immunoisolated transplantation. J Mater Sci Mater Med 2005;16(6):491–501.
[26] Igarashi T, Iwasaki N, Kasahara Y, Minami A. A cellular implantation system using an injectable ultra-purified alginate gel for repair of osteochondral defects in a rabbit model. J Biomed Mater Res A 2010;94(3):844–55.
[27] Sukegawa A, Iwasaki N, Kasahara Y, Onodera T, Igarashi T, Minami A. Repair of rabbit osteochondral defects by an acellular technique with an ultrapurified alginate gel containing stromal cell-derived factor-1. Tissue Eng Part A 2012;18(9–10):934–45.
[28] Baba R, Onodera T, Momma D, et al. A novel bone marrow stimulation technique augmented by administration of ultrapurified alginate gel enhances osteochondral repair in a rabbit model. Tissue Eng Part C Methods 2015;21(12):1263–73.
[29] Simpson NE, Stabler CL, Simpson CP, Sambanis A, Constantinidis I. The role of the CaCl2–guluronic acid interaction on alginate encapsulated βTC3 cells. Biomaterials 2004;25(13):2603–10.
[30] Rodrigues SA, Thambyah A, Broom ND. A multiscale structural investigation of the annulus-endplate anchorage system and its mechanisms of failure. Spine J 2015;15(3):405–16.
[31] Wade KR, Robertson PA, Thambyah A, Broom ND. "Surprise" loading in flexion increases the risk of disc herniation due to annulus-endplate junction failure: a mechanical and microstructural investigation. Spine (Phila Pa 1976) 2015;40(12):891–901.
[32] Pfirrmann CW, Metzdorf A, Zanetti M, Hodler J, Boos N. Magnetic resonance classification of lumbar intervertebral disc degeneration. Spine (Phila Pa 1976) 2001;26(17):1873–8.
[33] Sudo H, Yamada K, Iwasaki K, et al. Global identification of genes related to nutrient deficiency in intervertebral disc cells in an experimental nutrient deprivation model. PLoS One 2013;8(3):e58806.
[34] Masuda K, Sah RL, Hejna MJ, Thonar EJ. A novel two-step method for the formation of tissue-engineered cartilage by mature bovine chondrocytes: the alginate-recovered-chondrocyte (ARC) method. J Orthop Res 2003;21(1):139–48.
[35] Iwasaki K, Sudo H, Yamada K, Ito M, Iwasaki N. Cytotoxic effects of the radiocontrast agent iotrolan and anesthetic agents bupivacaine and lidocaine in three-dimensional cultures of human intervertebral disc nucleus pulposus cells: identification of the apoptotic pathways. PLoS One 2014;9(3):e92442.
[36] Iatridis JC, Weidenbaum M, Setton LA. Mow VC. Is the nucleus pulposus a solid or a fluid? Mechanical behaviors of the nucleus pulposus of the human intervertebral disc. Spine (Phila Pa 1976) 1996;21(10):1174–84.
[37] Sudo H, Oda I, Abumi K, Ito M, Kotani Y, Minami A. Biomechanical study on the effect of five different lumbar reconstruction techniques on adjacent-level intradiscal pressure and lamina strain. J Neurosurg Spine 2006;5(2):150–5.
[38] Sudo H, Oda I, Abumi K, et al. In vitro biomechanical effects of reconstruction on adjacent motion segment: comparison of aligned/kyphotic posterolateral fusion with aligned posterior lumbar interbody fusion/posterolateral fusion. J Neurosurg 2003;99(2 Suppl):221–8.
[39] Oehme D, Ghosh P, Shimmon S, et al. Mesenchymal progenitor cells combined with pentosan polysulfate mediating disc regeneration at the time of microdiscectomy: a preliminary study in an ovine model. J Neurosurg Spine 2014;20(6):657–69.
[40] O'Connell GD, Vresilovic EJ, Elliott DM. Comparison of animals used in disc research to human lumbar disc geometry. Spine (Phila Pa 1976) 2007;32(3):328–33.
[41] Hegewald AA, Medved F, Feng D, et al. Enhancing tissue repair in annulus fibrosus defects of the intervertebral disc: analysis of a bio-integrative annulus implant in an in-vivo ovine model. J Tissue Eng Regen Med 2015;9(4):405–14.
[42] Reitmaier S, Kreja L, Gruchenberg K, et al. In vivo biofunctional evaluation of hydrogels for disc regeneration. Eur Spine J 2014;23(1):19–26.
[43] Phillips FM, Tzermiadianos MN, Voronov LI, et al. Effect of the Total Facet Arthroplasty System after complete laminectomy-facetectomy on the biomechanics of implanted and adjacent segments. Spine J 2009;9(1):96–102.
[44] Russo F, Hartman RA, Bell KM, et al. Biomechanical evaluation of transpedicular nucleotomy with intact annulus fibrosus. Spine (Phila Pa 1976) 2017;42(4):E193–201.
[45] Wilke HJ, Neef P, Caimi M, Hoogland T, Claes LE. New in vivo measurements of pressures in the intervertebral disc in daily life. Spine (Phila Pa 1976) 1999;24(8):755–62.
[46] Beckstein JC, Sen S, Schaer TP, Vresilovic EJ, Elliott DM. Comparison of animal discs used in disc research to human lumbar disc: axial compression mechanics and glycosaminoglycan content. Spine (Phila Pa 1976) 2008;33(6):E166–73.
[47] Cunningham BW, Sefter JC, Shono Y, McAfee PC. Static and cyclical biomechanical analysis of pedicle screw spinal constructs. Spine (Phila Pa 1976) 1993;18(12):1677–88.
[48] Sakai D, Nakamura Y, Nakai T, et al. Exhaustion of nucleus pulposus progenitor cells with ageing and degeneration of the intervertebral disc. Nat Commun 2012;3:1264.
[49] Sakai D, Mochida J, Iwashina T, et al. Regenerative effects of transplanting mesenchymal stem cells embedded in atelocollagen to the degenerated intervertebral disc. Biomaterials 2006;27(3):335–45.
[50] Nishimura K, Mochida J. Percutaneous reinsertion of the nucleus pulposus. Exp Study Spine (Phila Pa 1976) 1998;23(14):1531–8 [discussion 9].
[51] Boos N, Weissbach S, Rohrbach H, Weiler C, Spratt KF, Nerlich AG. Classification of age-related changes in lumbar intervertebral discs: 2002 Volvo Award in basic science. Spine (Phila Pa 1976) 2002;27(23):2631–44.
[52] Ohta R, Kumagai F, Marumo H, Usumi K, Saito Y, Kuwagata M. Stress-reactive rats (high-avoidance female rats) have a shorter lifespan than stress-nonreactive rats (low-avoidance female rats). J Toxicol Pathol 2016;29(2):77–84.
[53] Goel VK, Panjabi MM, Patwardhan AG, et al. Test protocols for evaluation of spinal implants. J Bone Joint Surg Am 2006;88(Suppl. 2):103–9.
[54] Embree MC, Chen M, Pylawka S, et al. Exploiting endogenous fibrocartilage stem cells to regenerate cartilage and repair joint injury. Nat Commun 2016;7:13073.
[55] Shen W, Chen J, Zhu T, et al. Intra-articular injection of human meniscus stem/progenitor cells promotes meniscus regeneration and ameliorates osteoarthritis through stromal cell-derived factor-1/CXCR4-mediated homing. Stem Cells Transl Med 2014;3(3):387–94.
[56] Pelttari K, Pippenger B, Mumme M, et al. Adult human neural crest-derived cells for articular cartilage repair. Sci Transl Med 2014;6(251) [251ra119].
[57] Huey DJ, Hu JC, Athanasiou KA. Unlike bone, cartilage regeneration remains elusive. Science 2012;338(6109):917–21.
[58] Waskow C. Maintaining what is already there: strategies to rectify HSC transplantation dilemmas. Cell Stem Cell 2015;17(3):258–9.
[59] Sicari BM, Rubin JP, Dearth CL, et al. An acellular biologic scaffold promotes skeletal muscle formation in mice and humans with volumetric muscle loss. Sci Transl Med 2014;6(234):234ra58.
[60] Abbushi A, Endres M, Cabraja M, et al. Regeneration of intervertebral disc tissue by resorbable cell-free polyglycolic acid-based implants in a rabbit model of disc degeneration. Spine (Phila Pa 1976) 2008;33(14):1527–32.
[61] Lee KY, Mooney DJ. Alginate: properties and biomedical applications. Prog Polym Sci 2012;37(1):106–26.